Dipolar susceptibility of protein hydration shells

Salman Seyedi

Department of Physics, Arizona State University, PO Box 871504, Tempe, Arizona 85287

Dmitry V. Matyushov*

Department of Physics and School of Molecular Sciences, Arizona State University, PO Box 871504, Tempe, Arizona 85287

Abstract

We present a formalism for the calculation of interfacial dielectric constant of hydration shells of proteins from configurations produced by atomistic numerical simulations. The theoretical approach is applied to classical molecular dynamics simulations of hydrated cytochrome *c* protein in the range of temperatures from 280 to 330 K. The interfacial dielectric constant was found to be equal to 2–4 depending on temperature. This dielectric constant reflects constraints imposed by the protein on the hydration waters and their low ability to polarize in response to an external field.

Keywords: protein, hydration shell, dipolar susceptibility, dielectric constant, cytochrome

1. Introduction

Dielectric properties of hydrated proteins have been a subject of extensive studies for several decades, both experimentally [1, 2, 3, 4, 5] and computationally [6, 7, 8]. A part of the difficulty of the problem is a large number of relaxation processes and a wide range of relaxation times and corresponding dipolar responses. On slow time-scales of tens of nanoseconds, tumbling of a typically large (100-400 D [9]) protein dipole contributes to an increment of the dielectric constant of solution relative to bulk water. At shorter time-scales, one observes weak intermediate processes, often related to cross-correlations between the protein and water dipoles [6, 3]. This is followed by relaxation of bulk water at its corresponding Debye peak [10].

A completely separate set of issues related to the protein dielectric response appears when considering phenomena strongly affected by electrostatics of the protein and its environment. Those include most enzymatic reactions [11], shifts of pKa values of protein residues due to local electrostatic fields [12], spectral solvatochromism [13] and Stokes-shift dynamics [14, 15]. These problems require the knowledge of the average electrostatic potentials and fields inside the protein to determine the corresponding shifts of average energies recorded experimentally. Variances of electrostatic properties are also needed [7, 11, 16], in particular for describing protein electron transfer [7, 16], but those are accessible mostly from numerical atomistic simulations. All these problems, as well as issues related to protein-protein interactions and ionic effects on protein stability [17], call for the understanding of the structure [18] and dynamics [19] of water surrounding proteins.

The present report is focused on the analysis of the dipolar susceptibility of water in contact with the protein. Our goal is to establish and test a robust protocol for calculating such a susceptibility from atomistic simulations. A number of theoretical formalisms have been developed in the recent literature to address the question of the local polarization profile of water in contact with electrified substrates [20, 21, 22, 23, 24, 25, 26, 27] and proteins [8]. Most previous studies have focused on the local polarization of water dipoles in the interface, which, due to the layered structure of interfacial water [28, 29], exhibits large-amplitude oscillations [30]. Such a nonuniform distribution of polarization density prohibits defining a single corse-grained parameter quantifying the polarizability of the hydration shell. However, gauging polarizability of the interface is a pressing need, as has been recently demonstrated by measurements of the dielectric response of thin layers of water in contact with the graphite substrate [31]. The dielectric constant of interfacial water was reported

Email address: dmitrym@asu.edu (Dmitry V. Matyushov*)

to be ≈ 2 when restricted to the layer ≈ 1 nm thick [31]. Very similar values (≈ 3 – 9 depending on the solute size) were reported [32] from molecular dynamics (MD) simulations of model spherical nonpolar solutes in TIP3P [33] water.

The definition of the interface susceptibility used here and in previous simulations [32] is distinct from the models of the local dipolar response [21, 22, 25, 26]. We instead apply a coarse-graining protocol [34] to produce the surface polarity entering the electrostatic boundary-value problem and replacing the bulk dielectric constant used in standard formulations [35]. The dipolar susceptibility of the interface discussed below incorporates, in a coarse-grained fashion, the propensity of the interface to polarize when exposed to the field of external charges. Our application of this formalism to simulations of cytochrome c (cytC) protein has indeed produced a very low interfacial dielectric constant, ≈ 2 – 4, consistent with previous model simulations [34] and recent measurements [31].

2. Formalism

The electrostatic problem considered here is illustrated in Figure 1. We view a protein in solution as a repulsive core of complex shape, which expels the polar solvent (water) from its volume. The electric charges within the protein create the vacuum field $\mathbf{E}_0$, which depends on the overall distribution of molecular charge. The microscopic, instantaneous electric field in water outside the protein is $\mathbf{E}$. It is the sum of the field $\mathbf{E}_0$ of protein charges (considered as external or free charges in electrostatics [35]) and the field of the bound charges located at the atoms of the solvent. These bound charges have the charge density $\rho_b = -\nabla \cdot \mathbf{P}$, which is a scalar field equal to the divergence of the vector field $\mathbf{P}$ of the polarization density in the solvent [36]. The vector field $\mathbf{P}(\mathbf{r})$ thus represent the density of dipole moments of water at point $\mathbf{r}$ in the interface or in the bulk.

We now set up the projection $\hat{\mathbf{n}}$ normal to the dividing surface S at each point of the surface $\mathbf{r}_S$ and directed outward from the solvent (Figure 1). According to the Coulomb law, the difference of normal projections of the electric fields at the interface, the vacuum E_{0n} and the ensemble-averaged $\langle E_n \rangle$, is equal to the sum of densities of bound, σ_b, and free, σ_0, charges at the dividing surface [35]

$$E_{0n} - \langle E_n \rangle = 4\pi \left[\sigma_0 + \sigma_b \right]. \qquad (1)$$

Here, the surface density of the bound charge is given by the normal projection of the polarization density field

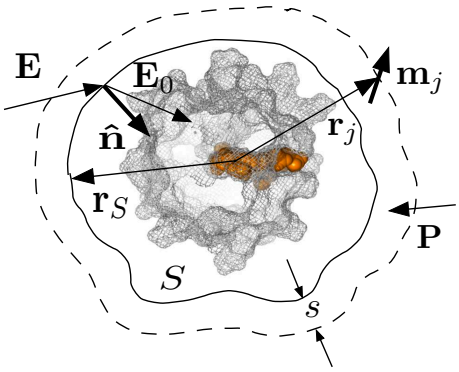

Figure 1: Schematics of electrostatic calculations performed for the hydration shell of cytochrome c. The dividing surface (solid line S) defines the normal unit vector $\hat{\mathbf{n}}(\mathbf{r}_S)$ specific to the point $\mathbf{r}_S$ at the dividing surface and directed outward from water. The electric field of protein charges inside the protein is $\mathbf{E}_0$; the combined field of protein charges and of the bound charges of water is the instantaneous electric field $\mathbf{E}$ inside the hydration shell. The vector field $\mathbf{P}$ is the density of water dipoles. The shell of thickness s around the protein is defined to calculate the dipole moment $M_n(s)$ in Eq. (4) by projecting each water dipole $\mathbf{m}_j$ on the local surface normal $\hat{\mathbf{n}}_j$. The heme of the protein is rendered orange.

taken at the dividing surface S

$$\sigma_b = \langle P_n \rangle = \langle \hat{\mathbf{n}} \cdot \mathbf{P} \rangle. \qquad (2)$$

In this equation, $P_n = P_n(\mathbf{r}_S) = \hat{\mathbf{n}}(\mathbf{r}_S) \cdot \mathbf{P}(\mathbf{r}_S)$ is an instantaneous polarization density at the position of the dividing surface $\mathbf{r}_S$ projected on the normal direction $\hat{\mathbf{n}}(\mathbf{r}_S)$ at the same point of the dividing surface (Figure 1). In contrast, $\langle P_n \rangle = \langle P_n(\mathbf{r}_S) \rangle$ is the normal projection of the polarization density averaged over all configurations of the protein-water system.

The normal projection of the polarization field is the only parameter of the interfacial electrostatics that enters the boundary-value problem solving for the electrostatic potential Φ of the protein-water system. The electrostatic potential inside the protein satisfies the Laplace equation, $\Delta\Phi = -4\pi\rho_0$, with the density of free charges ρ_0. Generally, $\langle P_n \rangle$ is the difference of dipolar field projections inside and outside of the protein, but we will assume that water has a significantly higher density of dipoles and is the only source of dipolar polarization in the interface. Therefore, $\langle P_n \rangle$ is assigned to water dipoles only.

According to the perturbation theory, the ensemble-averaged polarization created by the protein charges can be calculated from the binary correlation between the instantaneous normal polarization $\delta P_n = P_n - \langle P_n \rangle$ at the dividing surface and the potential energy of interaction $\delta U^{\mathrm{C}} = U^{\mathrm{C}} - \langle U^{\mathrm{C}} \rangle$ of the liquid with the atomic charges

of the protein [32, 34]

$$\langle P_n \rangle = -\beta \langle \delta P_n \delta U^{\mathrm{C}} \rangle. \tag{3}$$

Equation (3) in principle allows one to calculate the interfacial polarization from ensemble averages produced by numerical simulations. We, however, want to formulate the problem in terms of linear susceptibilities and will use a number of coarse graining approximations to arrive at a sufficiently general and robust definition of the dipolar susceptibility of the hydration shell.

One has to first recognize that the dividing surface between water and protein is not uniquely defined and $\langle P_n \rangle$ will show oscillations reflecting water's interfacial structure and depending on where the dividing surface has been chosen. The approach suggested in the past [34, 32] was to average these interfacial oscillations by calculating the total dipole moment $M_s(s)$ of the shell with the thickness s measured from the van der Waals surface of the protein

$$M_n(s) = \sum_{\mathbf{r}_j \in \mathrm{shell}} \mathbf{m}_j \cdot \hat{\mathbf{n}}_j. \tag{4}$$

Here, $\mathbf{m}_j$ are individual dipole moments of water molecules with coordinates of the oxygen atoms $\mathbf{r}_j$ (Figure 1). The water molecules with at least one of their atoms within the distance s from the closest protein atom were chosen to reside within the hydration shell of thickness s (Figure 1). Each dipole moment $\mathbf{m}_j$ was projected on the local normal $\hat{\mathbf{n}}_j$ calculated by locating a protein atom closest to the water molecule and using this direction as the normal to the surface.

Since the polarization density is the volume derivative of the dipole moment [35], one can coarse-grain the normal polarization projection at the dividing surface by taking the derivative with respect to the thickness s of the statistical correlation involving the total dipole moment of the shell

$$\langle \bar{P}_n \rangle = -\beta A^{-1} \frac{d}{ds} \left\langle \delta M_n(s) \delta U^{\mathrm{C}} \right\rangle. \tag{5}$$

Here, A is the surface area of the dividing surface. Further, in Eq. (5), we have done an additional step compared to the protocol adopted earlier [34, 32], where spherical geometries for the solutes were used. Since the geometry of the protein is non-spherical, the ensemble-averaged polarization $\langle P_n \rangle$ given by Eq. (3) depends on the position $\mathbf{r}_S$ at the dividing surface. Therefore, earlier protocols [34, 32] are not applicable here and additional coarse-graining is required. This is achieved with the coarse-grained $\langle \bar{P}_n \rangle$, which is the average of the normal polarization projection over both the interfacial oscillations, i.e., over different choices of the dividing surface, and over inhomogeneities at the protein surface, i.e., over different points $\mathbf{r}_S$ for each choice of the dividing surface.

The next step aims at formulating the problem in terms of interfacial susceptibilities. Since susceptibility of the interface should be related to the protein charge producing the electric $\mathbf{E}_0$, we replace U^{C} with the product of the solvent electrostatic potential ϕ_s with the total charge of the protein Q: $U^{\mathrm{C}} = Q\phi_s$, where $\phi_s = \sum_i (q_i/Q)\phi_{si}$ and the sum runs over all atomic charges q_i of the protein multiplied with the electrostatic potentials ϕ_{si} at their corresponding locations. Here, the entire set of ϕ_{si} needs to be evaluated at each protein-water configuration. We eliminate this computational difficulty by assigning Q and ϕ_s to the center of mass of the protein (the center of charge can be chosen instead, but usually produces very close results). Therefore, ϕ_s is the instantaneous, fluctuating electrostatic potential of water at the center of mass of the protein.

This approximation leads to a robust definition of the interface susceptibility as the ratio of $\langle \bar{P}_n \rangle$ and the surface-averaged normal-projected electric field of the protein charges $\langle \bar{E}_{0n} \rangle$

$$\chi_{0n} = \frac{\langle \bar{P}_n \rangle}{\langle \bar{E}_{0n} \rangle}. \tag{6}$$

The surface-averaged $\langle \bar{E}_{0n} \rangle$ is given, through the Gauss theorem [35], by the following relation

$$\langle \bar{E}_{0n} \rangle = A^{-1} \oint_A (\mathbf{E}_0 \cdot \hat{\mathbf{n}}) \, dA = -\frac{4\pi Q}{A}. \tag{7}$$

Combining these equations in Eq. (5), one obtains

$$\chi_{0n} = d\chi(s)/ds, \tag{8}$$

where

$$4\pi\chi(s) = \beta \langle \delta M_n(s) \delta\phi_s \rangle. \tag{9}$$

The interface susceptibility χ_{0n} carries the "0" subscript to stress that it is defined as a linear response to the field of the protein (free) charges $\langle \bar{E}_{0n} \rangle$. In contrast, the dielectric dipolar susceptibility is typically defined as the response to the ensemble-averaged Maxwell field $\langle \bar{E}_n \rangle$, which includes the field of the bound charges [35]. The susceptibility χ_{int} relating $\langle \bar{P}_n \rangle$ to $\langle \bar{E}_n \rangle$ as $\langle \bar{P}_n \rangle = \chi_{\mathrm{int}} \langle \bar{E}_n \rangle$ allows us to define the interface dielectric constant

$$\epsilon_{\mathrm{int}} - 1 = 4\pi\chi_{\mathrm{int}}. \tag{10}$$

One gets from Eq. (1)

$$\langle \bar{E}_{0n} \rangle - \langle \bar{E}_n \rangle = 4\pi \left[(Q_{\mathrm{surf}}/A) + \langle \bar{P}_n \rangle \right], \tag{11}$$

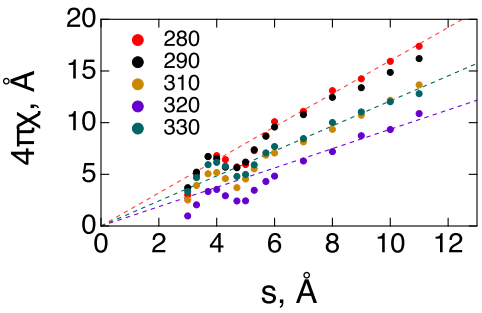

Figure 2: $4\pi\chi(s)$ (Eq. (9)) vs the thickness s of protein's hydration shell at different temperatures listed in the plot. The dashed lines are linear fits used to determine slopes in Eq. (8).

where $Q_{\rm surf}$ is the total surface charge of the protein. By substituting Eqs. (6) and (7) in this boundary condition, one obtains by rearranging terms

$$\epsilon_{\rm int} - 1 = \frac{4\pi\chi_{0n}}{1 + (Q_{\rm surf}/Q) - 4\pi\chi_{0n}}. \qquad (12)$$

Equation (12) is the main result of our formalism. Below, we will apply this protocol to configurations of the water-protein system produced by atomistic molecular dynamics (MD) simulations.

3. Results

The calculations of $\epsilon_{\rm int}$ were done based on MD trajectories produced for cytC protein (horse heart, PDB 1GIW). Classical, fully atomistic MD simulations at different temperatures were done as described elsewhere [37, 38, 39]. The simulation box contained one protein molecule solvated by 33231 TIP3P water molecules. NVT simulations with the trajectory length of 250 ns were carried out at each temperature after cooling/heating and equilibration from the equilibrated configuration at 300 K. Particle mesh Ewald was used to handle the long-range electrostatics, with the cutoff distance of 12.0 Å. The time step of 2.0 fs was used for all simulations.

The electrostatic potential produced by all water molecules in the simulation box was calculated at the nitrogen atom closest to protein's center of mass (NB in the heme, PDB 1GIW). This nitrogen atom turns out to be very close to the iron of the heme. The calculations presented here therefore produce the dipolar susceptibility of the protein-water interface required to calculate the average electrostatic potential of water at the heme by solving the dielectric boundary-value problem.

Figure 2 shows $4\pi\chi(s)$ calculated from Eq. (9) based on simulations of oxidized cytC ($Q = 9$) at different temperatures. The dashed lines indicate the linear interpolations used to determine the slope of $\chi(s)$ in Eq. (8). Despite some anticipated oscillations for narrow shells, reflecting water's interfacial structure, the adopted formalism offers a robust approach to calculate a coarse-grained dipolar susceptibility.

The calculations of $M_n(s)$ were truncated at $s \approx 11$ Å sufficient to produce the linear slope required for χ_{0s} in Eq. (8). The cross-correlations between the protein electrostatic field and water's dipoles can extend to larger distances of 20-40 Å into the bulk [40, 41]. Our truncation is therefore within the range of these long-range cross-correlations, which we do not consider here since our goal is limited to defining the dipolar susceptibility characterizing the interface of water with the protein.

The slopes obtained in Figure 2 are used in Eq. (12) to calculate $\epsilon_{\rm int}$ at different temperatures (Figure 3). This calculation requires defining the surface charge $Q_{\rm surf}$. Somewhat different results are obtained depending on the adopted protocol. Simple counting of the surface residues through VMD [42] leads to $Q_{\rm surf} = 11$. An alternative definition of the surface charge weighing each charge q_i of a water-exposed residue with its water-exposed area $A_i^{\rm exp}$ relative to the total area of the residue A_i (algorithm provided by Chimera [43]) leads to $Q_{\rm surf} = \sum_i q_i(A_i^{\rm exp}/A_i) = 9.7$. Both numbers are used to calculate $\epsilon_{\rm int}$ in Figure 3 through Eq. (12), and they yield slightly different results. We stress that $\epsilon_{\rm int}$ calculated here includes only the nuclear polarization accounted for by the non-polarizable TIP3P model. An additional interface susceptibility equal, as an estimate, to $\epsilon_\infty - 1$ should be added to $\epsilon_{\rm int}$ to incorporate the electronic and atomic polarization. Here, ϵ_∞ is the high-frequency dielectric constant of water [44], mostly related to electronic and atomic polarizabilities of the individual molecules. The effect of electronic polarizability in the interface might be more complex than this crude estimate since the effective dipole moment of water is expected to be lower in the interface compared to the bulk [45].

In contrast to the dielectric constant of bulk dielectrics [44] and to definitions of the protein dielectric constant based of fluctuations of the protein dipole moment [7], the interface dielectric constant $\epsilon_{\rm int}$ is not a direct gauge of the fluctuations of the dipole moment of water in the interface. The fluctuations of the dipole moment of hydration shells of nonpolar solutes [23, 24] are often enhanced compared to the bulk, following the local density profile in the interface [24]. In contrast,

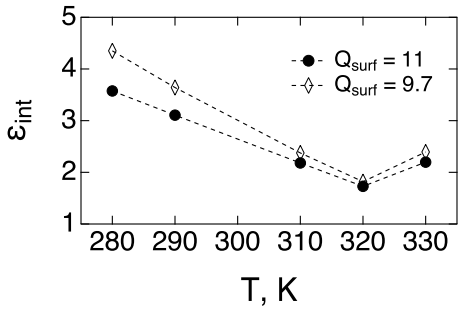

Figure 3: ϵ_{int} (Eq. (10)) vs T for oxidized cytochrome c with the total charge Q equal to 9. The calculations are done with the surface charge Q_{surf} equal to 9.7 (diamonds) and 11 (circles). The dashed lines connect the points to guide the eye.

fluctuations of the overall dipole of the protein hydration shell are reduced [8] compared to the bulk. The normal projection of the shell dipole on the surface normal, represented by ϵ_{int}, is further reduced compared to fluctuation of the overall shell dipole, leading to low values of ϵ_{int} reported here. Both effects reflect the frustrated, domain-like [46] arrangement of water in contact with charged and polar residues at the surface of the protein.

Low interface dielectric constant observed in our simulations does not represent the dielectric constant of the bulk. In solid materials, and in dielectric models representing solid dielectrics [35], the surface polarization $\langle P_n \rangle$ is linked to the bulk dielectric constant. This is because a solid dielectric maintains bulk stress, which propagates to the surface in the form of surface polarization and the corresponding surface charge density. This picture goes back to Maxwell who viewed a solid dielectric as two oppositely-charged liquids which can be shifted relative to each other through the bulk stress caused by an external electric field [47]. The ability to maintain bulk stress is central to this argument allowing propagation of a bulk property to the interface. Liquids do not maintain bulk stress, and the surface polarization represents only a thin interfacial layer of molecular scale [30, 34, 31]. The interface susceptibility calculated here is a property of this thin interfacial layer, which does not apply to the bulk. In contrast, the bulk dielectric response develops from mutual orientational correlations of dipoles in the liquid [44] represented by chains of dipolar correlations with long-ranged, $\propto r^{-3}$, distance decay [48]. The bulk dielectric constant, as a measure of dielectric screening and liquid polarity, arises from accumulation of these correlations over distances larger than molecular scale. Interface prevents accumulation of dielectric screening: geometric and energetic constrains in the interface frustrate the dipoles and break their long-range correlations, effectively leading to a reduced interface susceptibility.

4. Conclusions

Water in the hydration shell of a protein is highly perturbed from the bulk through the combination of local electrostatic fields of ionized surface residues, hydrogen bonds to the protein, and mutual frustration of dipoles in the geometrically constrained interfacial layer. Despite high degree of the dynamic and static disorder of the protein hydration shell [8, 49], the dipolar response in the direction normal to the dividing surface is strongly restricted. The result is a very low effective dielectric constant of the hydration layer (Figure 3). This effective dielectric constant enters the electrostatic boundary-value problem and thus determines the average electrostatic potential inside the protein.

The precise physical origin of the low susceptibility of the interface is not easy to establish. Electric fields are strong at the protein surface, but much weaker fields, $\approx 7 \times 10^5$ V/cm, were applied in experiments [31] with thinnest water layers available for measurements and yielding $\epsilon_{int} \approx 2$. Simulations indicate that a low interface dielectric constant remains essentially unchanged between ionic and neutral solutes [32]. This simulation evidence, combined with experimental observations [31], allows us to suggest that the main cause of the weak dipolar response is through geometrical constraints preventing large-amplitude reorientations of the interfacial dipoles in and out of the normal direction.

The dipolar response of the interface is very different from the bulk and that should lead to a number of observable consequences linked to the interfacial polarization being qualitatively and quantitatively different from the predictions of the standard dielectric boundary-value problem [35]. Absorption of radiation by protein solutions does not follow the recipe of Maxwell's electrostatics and instead can be formulated in terms of the Lorentz virtual cavity [41]. Along similar lines, the force experienced by a protein in a nonuniform electric field (dielectrophoresis) turns out to be three-four orders of magnitude higher [50] than what follows from the typically used Clausius-Mossotti factor. How all these effects combine to allow specific orientations of the protein under the influence of strong electric fields in the intracellular environment remains an open question.

Notes

The authors declare no competing financial interest.

Acknowledgements

This research was supported by the National Science Foundation (CHE-1800243). CPU time was provided by the National Science Foundation through XSEDE resources (TG-MCB080071).

[1] E. H. Grant, R. J. Sheppard, G. P. South, Dielectric Behaviour of Biological Molecules in Solution, Clarendon Press, Oxford, 1978.

[2] R. Pethig, Protein-water interactions determined by dielectric methods, Annu. Rev. Phys. Chem. 43 (1992) 177–205.

[3] A. Oleinikova, P. Sasisanker, H. Weingärtner, What can really be learned from dielectric spectroscopy of protein solutions? a case study of Ribonuclease A, J. Phys. Chem. B 108 (2004) 8467.

[4] C. Cametti, S. Marchetti, C. M. C. Gambi, G. Onori, Dielectric relaxation spectroscopy of lysozyme aqueous solutions: Analysis of the delta-dispersion and the contribution of the hydration water, J. Phys. Chem. B 115 (21) (2011) 7144–7153.

[5] K. L. Ngai, S. Capaccioli, A. Paciaroni, Dynamics of hydrated proteins and bio-protectants: Caged dynamics, β-relaxation, and α-relaxation, Biochim. Biophys. Acta (BBA) - General Subjects 1861 (1) (2017) 3553–3563.

[6] S. Boresch, P. Höchtl, O. Steinhauser, Studying the dielectric properties of a protein solution by computer simulation, J. Phys. Chem. B 104 (2000) 8743.

[7] T. Simonson, Electrostatics and dynamics of proteins, Rep. Prog. Phys. 66 (2003) 737–787.

[8] S. Mukherjee, S. Mondal, B. Bagchi, Distinguishing dynamical features of water inside protein hydration layer: Distribution reveals what is hidden behind the average, J. Chem. Phys. 147 (2) (2017) 024901–13.

[9] S. Takashima, Electric dipole moment of globular proteins: measurement and calculation with NMR and X-ray databases, J. Noncrystal. Solids 305 (2002) 303–310.

[10] N. Q. Vinh, M. S. Sherwin, S. J. Allen, D. K. George, A. J. Rahmani, K. W. Plaxco, High-precision gigahertz-to-terahertz spectroscopy of aqueous salt solutions as a probe of the femtosecond-to-picosecond dynamics of liquid water, J. Chem. Phys. 142 (16) (2015) 164502–8.

[11] A. Warshel, P. K. Sharma, M. Kato, Y. Xiang, H. Liu, M. H. M. Olsson, Electrostatic basis for enzyme catalysis, Chem. Rev. 106 (8) (2006) 3210–3235. doi:10.1021/cr0503106.

[12] J. Antosiewicz, J. A. McCammon, M. K. Gilson, Prediction of pH-dependent properties of proteins, J. Molec. Biol. 238 (3) (1994) 415–436.

[13] S. H. Schneider, S. G. Boxer, Vibrational Stark effects of carbonyl probes applied to reinterpret IR and Raman data for enzyme inhibitors in terms of electric fields at the active site, J. Phys. Chem. B 120 (36) (2016) 9672–9684.

[14] X. J. Jordanides, M. J. Lang, X. Song, G. R. Fleming, Solvation dynamics in protein environments studied by photon echo spectroscopy, J. Phys. Chem. B 103 (1999) 7995–8005.

[15] R. Biswas, B. Bagchi, Anomalous water dynamics at surfaces and interfaces: synergistic effects of confinement and surface interactions, J. Phys.: Condens. Matter 30 (1) (2018) 013001–27.

[16] D. V. Matyushov, Protein electron transfer: is biology (thermo)dynamic?, J. Phys.: Condens. Matter 27 (47) (2015) 473001.

[17] H.-X. Zhou, X. Pang, Electrostatic interactions in protein structure, folding, binding, and condensation, Chem. Rev. 118 (4) (2018) 1691–1741.

[18] M.-C. Bellissent-Funel, A. Hassanali, M. Havenith, R. Henchman, P. Pohl, F. Sterpone, D. van der Spoel, Y. Xu, A. E. García, Water determines the structure and dynamics of proteins, Chem. Rev. 116 (13) (2016) 7673–7697.

[19] D. Laage, T. Elsaesser, J. T. Hynes, Water dynamics in the hydration shells of biomolecules., Chem. Rev. 117 (16) (2017) 10694–10725.

[20] I.-C. Yeh, M. L. Berkowitz, Dielectric constant of water at high electric fields: Molecular dynamics study, J. Chem. Phys. 110 (16) (1999) 7935–7942.

[21] H. A. Stern, S. E. Feller, Calculation of the dielectric permittivity profile for a nonuniform system: Application to a lipid bilayer simulation, J. Chem. Phys. 118 (7) (2003) 3401–3412.

[22] V. Ballenegger, J.-P. Hansen, Dielectric permittivity profiles of confined polar liquids, J. Chem. Phys. 122 (2005) 114711.

[23] J. Martí, G. Nagy, E. Guàrdia, M. C. Gordillo, Molecular Dynamics Simulation of Liquid Water Confined inside Graphite Channels: Dielectric and Dynamical Properties, J. Phys. Chem. B 110 (47) (2006) 23987–23994.

[24] A. D. Friesen, D. V. Matyushov, Local polarity excess at the interface of water with a nonpolar solute, Chem. Phys. Lett. 511 (2011) 256–261.

[25] S. Gekle, R. R. Netz, Anisotropy in the dielectric spectrum of hydration water and its relation to water dynamics, J. Chem. Phys. 137 (10) (2012) 104704–12.

[26] A. Schlaich, E. W. Knapp, R. R. Netz, Water dielectric effects in planar confinement, Phys. Rev. Lett. 117 (4) (2016) 048001.

[27] B. Shi, M. V. Agnihotri, S.-H. Chen, R. Black, S. J. Singer, Polarization charge: Theory and applications to aqueous interfaces, J. Chem. Phys. 144 (16) (2016) 164702.

[28] J.-J. Velasco-Velez, C. H. Wu, T. A. Pascal, L. F. Wan, J. Guo, D. Prendergast, M. Salmeron, Interfacial water. The structure of interfacial water on gold electrodes studied by x-ray absorption spectroscopy., Science 346 (6211) (2014) 831–834.

[29] L. S. Pedroza, P. Brandimarte, A. R. Rocha, M. V. Fernández-Serra, Bias-dependent local structure of water molecules at a metallic interface, Chem. Sci. 9 (1) (2018) 62–69.

[30] L. Horváth, T. Beu, M. Manghi, J. Palmeri, The vapor-liquid interface potential of (multi)polar fluids and its influence on ion solvation, J. Chem. Phys. 138 (15) (2013) 154702.

[31] L. Fumagalli, A. Esfandiar, R. Fabregas, S. Hu, P. Ares, A. Janardanan, Q. Yang, B. Radha, T. Taniguchi, K. Watanabe, G. Gomila, K. S. Novoselov, A. K. Geim, Anomalously low dielectric constant of confined water, Science 360 (6395) (2018) 1339–1342.

[32] M. Dinpajooh, D. V. Matyushov, Dielectric constant of water in the interface, J. Chem. Phys. 145 (2016) 014504.

[33] W. L. Jorgensen, J. Chandrasekhar, J. D. Madura, R. W. Impey, M. L. Klein, Comparison of simple potential functions for simulating liquid water, J. Chem. Phys. 79 (2) (1983) 926–935.

[34] D. V. Matyushov, Electrostatics of liquid interfaces, J. Chem. Phys. 140 (2014) 224506.

[35] J. D. Jackson, Classical Electrodynamics, Wiley, New York, 1999.

[36] L. D. Landau, E. M. Lifshitz, Electrodynamics of Continuous Media, Pergamon, Oxford, 1984.

[37] M. Dinpajooh, D. R. Martin, D. V. Matyushov, Polarizability of the active site of cytochrome *c* reduces the activation barrier for electron transfer, Sci. Rep. 6 (2016) 28152.

[38] S. Seyedi, M. M. Waskasi, D. V. Matyushov, Theory and electrochemistry of cytochrome *c*, J. Phys. Chem. B 121 (2017) 4958–4967.

[39] S. Seyedi, D. V. Matyushov, Termination of biological function at low temperatures: Glass or structural transition?, J. Phys. Chem. Lett. 9 (2018) 2359–2366.

[40] D. V. Matyushov, Dipolar response of hydrated proteins, J. Chem. Phys. 136 (2012) 085102.

[41] D. R. Martin, D. V. Matyushov, Terahertz absorption of lysozyme in solution, J. Chem. Phys. 146 (2017) 084502.

[42] W. Humphrey, A. Dalke, K. Schulten, VMD - visual molecular dynamics, J. Molec. Graphics 14 (1) (1996) 33–38.
[43] E. F. Pettersen, T. D. Goddard, C. C. Huang, G. S. Couch, D. M. Greenblatt, E. C. Meng, T. E. Ferrin, Ucsf chimera – a visualization system for exploratory research and analysis, J. Comput. Chem. 13 (2004) 1605–1612.
[44] C. J. F. Böttcher, Theory of Electric Polarization, Vol. 1: Dielectrics in Static Fields, Elsevier, Amsterdam, 1973.
[45] F. S. Cipcigan, V. P. Sokhan, A. P. Jones, J. Crain, G. J. Martyna, Hydrogen bonding and molecular orientation at the liquid–vapour interface of water, Phys. Chem. Chem. Phys. 17 (14) (2015) 8660–8669.
[46] D. R. Martin, D. V. Matyushov, Dipolar nanodomains in protein hydration shells, J. Phys. Chem. Lett. 6 (3) (2015) 407–412.
[47] J. C. Maxwell, A Treatise on Electricity and Magnetism, Vol. 1, Dover Publications, New York, 1954, sec. 63.
[48] J. S. Høye, G. Stell, Statistical mechanics of polar systems: Dielectric constant for dipolar fluids, J. Chem. Phys. 61 (1974) 562.
[49] D. R. Martin, J. E. Forsmo, D. V. Matyushov, Complex dynamics of water in protein confinement, J. Phys. Chem. B 122 (13) (2018) 3418–3425.
[50] S. S. Seyedi, D. V. Matyushov, Protein Dielectrophoresis in Solution, J. Phys. Chem. B 122 (39) (2018) 9119–9127.